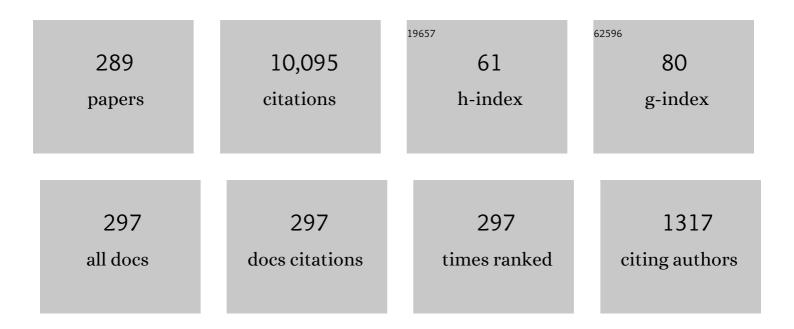
Huseyin O Tekin

List of Publications by Year in descending order

Source: https://exaly.com/author-pdf/2872580/publications.pdf Version: 2024-02-01



#	Article	IF	CITATIONS
1	Effects of micro-sized and nano-sized WO 3 on mass attenauation coefficients of concrete by using MCNPX code. Applied Radiation and Isotopes, 2017, 121, 122-125.	1.5	170
2	An extensive investigation on gamma ray shielding features of Pd/Ag-based alloys. Nuclear Engineering and Technology, 2019, 51, 853-859.	2.3	165
3	Shielding features of concrete types containing sepiolite mineral: Comprehensive study on experimental, XCOM and MCNPX results. Results in Physics, 2018, 11, 40-45.	4.1	127
4	Gamma radiation shielding properties of the hematite-serpentine concrete blended with WO3 and Bi2O3 micro and nano particles using MCNPX code. Radiation Physics and Chemistry, 2018, 150, 95-100.	2.8	126
5	Investigation of structural, thermal properties and shielding parameters for multicomponent borate glasses for gamma and neutron radiation shielding applications. Journal of Non-Crystalline Solids, 2017, 471, 222-237.	3.1	124
6	Amorphous alloys with high Fe content for radiation shielding applications. Radiation Physics and Chemistry, 2021, 183, 109386.	2.8	123
7	Investigations of radiation shielding using Monte Carlo method and elastic properties of PbO-SiO2-B2O3-Na2O glasses. Current Applied Physics, 2018, 18, 717-727.	2.4	118
8	Structure, optical, gamma-ray and neutron shielding properties of NiO doped B2O3–BaCO3–Li2O3 glass systems. Ceramics International, 2020, 46, 1711-1721.	4.8	117
9	Gamma, neutron shielding and mechanical parameters for lead vanadate glasses. Ceramics International, 2019, 45, 14058-14072.	4.8	116
10	Influence of Bi2O3 concentration on barium-telluro-borate glasses: Physical, structural and radiation-shielding properties. Ceramics International, 2021, 47, 329-340.	4.8	110
11	Optical properties and gamma-shielding features of bismuth borate glasses. Applied Physics A: Materials Science and Processing, 2018, 124, 1.	2.3	106
12	Comparative study of gamma-ray shielding and elastic properties of BaO–Bi2O3–B2O3 and ZnO–Bi2O3–B2O3 glass systems. Materials Chemistry and Physics, 2018, 217, 11-22.	4.0	102
13	The Mass stopping power / projected range and nuclear shielding behaviors of barium bismuth borate glasses and influence of cerium oxide. Ceramics International, 2019, 45, 15348-15357.	4.8	102
14	Evaluation of gamma-ray and neutron shielding features of heavy metals doped Bi2O3-BaO-Na2O-MgO-B2O3 glass systems. Progress in Nuclear Energy, 2020, 118, 103118.	2.9	102
15	Radiation shielding and mechanical properties of Al2O3-Na2O-B2O3-Bi2O3 glasses using MCNPX Monte Carlo code. Materials Chemistry and Physics, 2019, 223, 209-219.	4.0	101
16	Shielding properties of 80TeO2–5TiO2–(15â^'x) WO3–xAnOm glasses using WinXCom and MCNP5 code. Radiation Physics and Chemistry, 2017, 141, 172-178.	2.8	98
17	Estimation of gamma radiation shielding qualification of newly developed glasses by using WinXCOM and MCNPX code. Progress in Nuclear Energy, 2019, 115, 12-20.	2.9	97
18	Simulation of shielding parameters for TeO2-WO3-GeO2 glasses using FLUKA code. Results in Physics, 2019, 13, 102199.	4.1	95

#	Article	IF	CITATIONS
19	Alteration of optical, structural, mechanical durability and nuclear radiation attenuation properties of barium borosilicate glasses through BaO reinforcement: Experimental and numerical analyses. Ceramics International, 2021, 47, 5587-5596.	4.8	95
20	A comparative study on gamma photon shielding features of various germanate glass systems. Composites Part B: Engineering, 2019, 165, 636-647.	12.0	94
21	Investigation of photon shielding performances of some selected alloys by experimental data, theoretical and MCNPX code in the energy range of 81†keV†1333†keV. Journal of Alloys and Compounds, 2019, 772, 516-524.	5.5	94
22	Characterization of SiO2–PbO–CdO–Ga2O3 glasses for comprehensive nuclear shielding performance: Alpha, proton, gamma, neutron radiation. Ceramics International, 2019, 45, 19206-19222.	4.8	93
23	Experimental studies and Monte Carlo simulations on gamma ray shielding competence of (30+x)PbO 10WO3 10Na2O â^ 10MgO – (40-x)B2O3 glasses. Progress in Nuclear Energy, 2020, 119, 103047.	2.9	93
24	ZnO-B2O3-PbO glasses: Synthesis and radiation shielding characterization. Physica B: Condensed Matter, 2018, 548, 20-26.	2.7	92
25	Photon and neutron shielding performance of boron phosphate glasses for diagnostic radiology facilities. Results in Physics, 2019, 12, 1457-1464.	4.1	92
26	Nuclear radiation shielding using barium borosilicate glass ceramics. Journal of Physics and Chemistry of Solids, 2020, 142, 109437.	4.0	92
27	Effect of Bi2O3 content on mechanical and nuclear radiation shielding properties of Bi2O3-MoO3-B2O3-SiO2-Na2O-Fe2O3 glass system. Results in Physics, 2019, 13, 102165.	4.1	91
28	Photon shielding characterizations of bismuth modified borate –silicate–tellurite glasses using MCNPX Monte Carlo code. Materials Chemistry and Physics, 2018, 211, 9-16.	4.0	89
29	Radiation shielding study of tellurite tungsten glasses with different antimony oxide as transparent shielding materials using MCNPX code. Journal of Non-Crystalline Solids, 2018, 498, 167-172.	3.1	89
30	Structural, UV and shielding properties of ZBPC glasses. Journal of Non-Crystalline Solids, 2019, 509, 99-105.	3.1	89
31	Radiation shielding features using MCNPX code and mechanical properties of the PbO Na2O B2O3CaO Al2O3SiO2 glass systems. Composites Part B: Engineering, 2019, 167, 231-240.	12.0	89
32	Comparative investigations of gamma and neutron radiation shielding parameters for different borate and tellurite glass systems using WinXCom program and MCNPX code. Materials Chemistry and Physics, 2018, 215, 183-202.	4.0	88
33	FTIR, electronic polarizability and shielding parameters of B2O3 glasses doped with SnO2. Applied Physics A: Materials Science and Processing, 2018, 124, 1.	2.3	87
34	Evaluation of the shielding parameters of alkaline earth based phosphate glasses using MCNPX code. Results in Physics, 2019, 12, 101-106.	4.1	87
35	Photon attenuation coefficients of different rock samples using MCNPX, Geant4 simulation codes and experimental results: a comparison study. Radiation Effects and Defects in Solids, 2018, 173, 900-914.	1.2	86
36	An investigation on shielding properties of BaO, MoO3 and P2O5 based glasses using MCNPX code. Results in Physics, 2019, 12, 629-634.	4.1	85

#	Article	IF	CITATIONS
37	MCNP-X Monte Carlo Code Application for Mass Attenuation Coefficients of Concrete at Different Energies by Modeling 3 × 3 Inch NaI(Tl) Detector and Comparison with XCOM and Monte Carlo Data. Science and Technology of Nuclear Installations, 2016, 2016, 1-7.	0.8	84
38	Experimental investigation of photon attenuation behaviors for concretes including natural perlite mineral. Results in Physics, 2019, 12, 237-243.	4.1	84
39	The influence of gallium (Ga) additive on nuclear radiation shielding effectiveness of Pd/Mn binary alloys. Journal of Alloys and Compounds, 2020, 815, 152484.	5.5	84
40	The impact of Cr2O3 additive on nuclear radiation shielding properties of LiF–SrO–B2O3 glass system. Materials Chemistry and Physics, 2020, 242, 122481.	4.0	83
41	The investigation of gamma-ray and neutron shielding parameters of Na2O-CaO-P2O5-SiO2 bioactive glasses using MCNPX code. Results in Physics, 2019, 12, 1797-1804.	4.1	81
42	Er2O3 effects on photon and neutron shielding properties of TeO2-Li2O-ZnO-Nb2O5 glass system. Results in Physics, 2019, 13, 102277.	4.1	80
43	Influence of Bi2O3/WO3 substitution on the optical, mechanical, chemical durability and gamma ray shielding properties of lithium-borate glasses. Ceramics International, 2021, 47, 5286-5299.	4.8	80
44	A comprehensive study of the energy absorption and exposure buildup factors of different bricks for gamma-rays shielding. Results in Physics, 2017, 7, 2528-2533.	4.1	79
45	An extensive investigation on gamma-ray and neutron attenuation parameters of cobalt oxide and nickel oxide substituted bioactive glasses. Ceramics International, 2019, 45, 9934-9949.	4.8	78
46	Radiological parameters of bismuth oxide glasses using the Phy-X/PSD software. Emerging Materials Research, 2020, 9, 1020-1027.	0.7	76
47	Nuclear radiation shielding competences of barium-reinforced borosilicate glasses. Emerging Materials Research, 2020, 9, 1131-1144.	0.7	75
48	The multiple characterization of gamma, neutron and proton shielding performances of xPbO-(99-x)B2O3–Sm2O3 glass system. Ceramics International, 2019, 45, 23561-23571.	4.8	74
49	Physical and nuclear shielding properties of newly synthesized magnesium oxide and zinc oxide nanoparticles. Nuclear Engineering and Technology, 2020, 52, 2078-2084.	2.3	74
50	The direct effect of Er ₂ O ₃ on bismuth barium telluro borate glasses for nuclear security applications. Materials Research Express, 2019, 6, 115212.	1.6	73
51	The effective contribution of PbO on nuclear shielding properties of xPbO-(100 â^ x)P2O5 glass system: broad range investigation. Applied Physics A: Materials Science and Processing, 2019, 125, 1.	^a 2.3	72
52	An Investigation on Radiation Protection and Shielding Properties of 16 Slice Computed Tomography (CT) Facilities. International Journal of Computational and Experimental Science and Engineering, 2018, 4, 37-40.	10.0	71
53	Simulations of mass attenuation coefficients for shielding materials using the MCNP-X code. Nuclear Science and Techniques/Hewuli, 2017, 28, 1.	3.4	69
54	Synthesis and nuclear radiation shielding characterization of newly developed germanium oxide and bismuth oxide glasses. Ceramics International, 2019, 45, 24664-24674.	4.8	69

#	Article	IF	CITATIONS
55	Bioactive glasses and direct effect of increased K2O additive for nuclear shielding performance: A comparative investigation. Ceramics International, 2020, 46, 1323-1333.	4.8	68
56	Structural, mechanical and radiation shielding properties of newly developed tungsten lithium borate glasses: An experimental study. Journal of Non-Crystalline Solids, 2020, 532, 119882.	3.1	68
57	Synthesis, optical, structural and physical properties of newly developed dolomite reinforced borate glasses for nuclear radiation shielding utilizations: An experimental and simulation study. Optical Materials, 2021, 114, 110942.	3.6	68
58	New transparent rare earth glasses for radiation protection applications. Applied Physics A: Materials Science and Processing, 2019, 125, 1.	2.3	67
59	SnO-reinforced silicate glasses and utilization in gamma-radiation-shielding applications. Emerging Materials Research, 2020, 9, 1000-1008.	0.7	67
60	New approach to removal of hazardous Bypass Cement Dust (BCD) from the environment: 20Na2O-20BaCl2-(60-x)B2O3-(x)BCD glass system and Optical, mechanical, structural and nuclear radiation shielding competences. Journal of Hazardous Materials, 2021, 403, 123738.	12.4	66
61	Binary B2O3–Bi2O3 glasses: scrutinization of directly and indirectly ionizing radiations shielding abilities. Journal of Materials Research and Technology, 2020, 9, 14549-14567.	5.8	63
62	Effect of CdO addition on photon, electron, and neutron attenuation properties of boro-tellurite glasses. Ceramics International, 2021, 47, 5951-5958.	4.8	63
63	Investigations on borate glasses within SBC-Bx system for gamma-ray shielding applications. Nuclear Engineering and Technology, 2021, 53, 282-293.	2.3	62
64	MoO ₃ -TeO ₂ glass system for gamma ray shielding applications. Materials Research Express, 2020, 7, 025202.	1.6	60
65	Synthesis, structure, optical and gamma radiation shielding properties of B2O3-PbO2-Bi2O3 glasses. Composites Part B: Engineering, 2019, 172, 218-225.	12.0	59
66	Newly developed tellurium oxide glasses for nuclear shielding applications: An extended investigation. Journal of Non-Crystalline Solids, 2020, 528, 119763.	3.1	56
67	Synthesis, physical, optical, mechanical, and radiation attenuation properties of TiO2–Na2O–Bi2O3–B2O3 glasses. Ceramics International, 2021, 47, 185-204.	4.8	55
68	Role of heavy metal oxides on the radiation attenuation properties of newly developed TBBE-X glasses by computational methods. Physica Scripta, 2021, 96, 075302.	2.5	55
69	Assessment of the Willingness of Radiologists and Radiographers to Accept the Integration of Artificial Intelligence Into Radiology Practice. Academic Radiology, 2022, 29, 87-94.	2.5	54
70	Radiation shielding properties of pentaternary borate glasses using MCNPX code. Journal of Physics and Chemistry of Solids, 2018, 121, 17-21.	4.0	53
71	Characterization of a broad range gamma-ray and neutron shielding properties of MgO-Al2O3-SiO2-B2O3 and Na2O-Al2O3-SiO2 glass systems. Journal of Non-Crystalline Solids, 2019, 518, 92-102.	3.1	53
72	Multi-objective optimization strategies for radiation shielding performance of BZBB glasses using Bi2O3: A FLUKA Monte Carlo code calculations. Journal of Materials Research and Technology, 2020, 9, 12335-12345.	5.8	53

#	Article	IF	CITATIONS
73	MCNPX Simulation for Radiation Dose Absorption of Anatomical Regions and Some Organs. Acta Physica Polonica A, 2020, 137, 561-565.	0.5	53
74	Ytterbium (III) oxide reinforced novel TeO2–B2O3–V2O5 glass system: Synthesis and optical, structural, physical and thermal properties. Ceramics International, 2021, 47, 18517-18531.	4.8	52
75	Newly developed Zinc-Tellurite glass system: An experimental investigation on impact of Ta2O5 on nuclear radiation shielding ability. Journal of Non-Crystalline Solids, 2020, 544, 120169.	3.1	51
76	Enhancement of nuclear radiation shielding and mechanical properties of YBiBO3 glasses using La2O3. Nuclear Engineering and Technology, 2020, 52, 1297-1303.	2.3	50
77	The influence of heavy elements on the ionizing radiation shielding efficiency and elastic properties of some tellurite glasses: Theoretical investigation. Results in Physics, 2020, 19, 103496.	4.1	50
78	Photon and neutron shielding characteristics of samarium doped lead alumino borate glasses containing barium, lithium and zinc oxides determined at medical diagnostic energies. Results in Physics, 2019, 12, 2123-2128.	4.1	49
79	Gamma shielding and compressive strength analyses of polyester composites reinforced with zinc: an experiment, theoretical, and simulation based study. Applied Physics A: Materials Science and Processing, 2020, 126, 1.	2.3	49
80	Structural and nuclear radiation shielding properties of bauxite ore doped lithium borate glasses: Experimental and Monte Carlo study. Radiation Physics and Chemistry, 2019, 162, 187-193.	2.8	47
81	Improvement of mechanical properties and radiation shielding performance of AlBiBO3 glasses using yttria: An experimental investigation. Ceramics International, 2020, 46, 3534-3542.	4.8	47
82	Investigation of radiation shielding properties for Bi2O3 - V2O5 - TeO2 glass system using MCNP5 code. Journal of Non-Crystalline Solids, 2018, 499, 32-40.	3.1	46
83	Gamma photon and neutron attenuation properties of MgO–BaO–B2O3–TeO2–Cr2O3 glasses: The role of TeO2. Radiation Physics and Chemistry, 2019, 163, 58-66.	2.8	46
84	Fabrication, FTIR, physical characteristics and photon shielding efficacy of CeO2 /sand reinforced borate glasses: Experimental and simulation studies. Radiation Physics and Chemistry, 2022, 191, 109837.	2.8	46
85	Physical, structural, and radiation shielding properties of B2O3–MgO–K2O–Sm2O3 glass network modified with TeO2. Radiation Physics and Chemistry, 2019, 160, 75-82.	2.8	45
86	A comprehensive study on novel alumino-borosilicate glass reinforced with Bi2O3 for radiation shielding applications: synthesis, spectrometer, XCOM, and MCNP-X works. Journal of Materials Science: Materials in Electronics, 2021, 32, 13882-13896.	2.2	45
87	A detailed investigation on highly dense CuZr bulk metallic glasses for shielding purposes. Open Chemistry, 2022, 20, 69-80.	1.9	45
88	A journey for exploration of Eu2O3 reinforcement effect on zinc-borate glasses: Synthesis, optical, physical and nuclear radiation shielding properties. Ceramics International, 2021, 47, 2572-2583.	4.8	44
89	Charged particles and gamma-ray shielding features of oxyfluoride semiconducting glasses: TeO2-Ta2O5-ZnO/ZnF2. Ceramics International, 2020, 46, 25035-25042.	4.8	43
90	Calculation of Detection Efficiency for the Gamma Detector using MCNPX. Acta Physica Polonica A, 2015, 128, B-332-B-335.	0.5	43

#	Article	IF	CITATIONS
91	Shielding behaviour of (20â€⁻+â€⁻x) Bi2O3 – 20BaO–10Na2O–10MgO–(40-x) B2O3: An experimental ar Carlo study. Chemical Physics, 2020, 529, 110571.	nd Monte	42
92	The radiology workforce's response to the COVID-19 pandemic in the Middle East, North Africa and India. Radiography, 2021, 27, 360-368.	2.1	41
93	Nuclear shielding properties of B2O3–Pb3O4–ZnO glasses: Multiple impacts of Er2O3 additive. Ceramics International, 2020, 46, 27849-27859.	4.8	40
94	Structural and physical characterization study on synthesized tellurite (TeO2) and germanate (GeO2) glass shields using XRD, Raman spectroscopy, FLUKA and PHITS. Optical Materials, 2020, 110, 110533.	3.6	40
95	The impact of samarium (III) oxide on structural, optical and radiation shielding properties of thallium-borate glasses: Experimental and numerical investigation. Optical Materials, 2021, 114, 110948.	3.6	40
96	Synergistic effect of La2O3 on mass stopping power (MSP)/projected range (PR) and nuclear radiation shielding abilities of silicate glasses. Results in Physics, 2019, 14, 102424.	4.1	39
97	Correlate the structural changes to gamma radiation shielding performance evaluation for some calcium bismuth-borate glasses containing Nb2O5. Physica B: Condensed Matter, 2019, 567, 109-112.	2.7	39
98	Physical, neutron, and gamma-rays shielding parameters for Na ₂ O–SiO ₂ –PbO glasses. Emerging Materials Research, 2021, 10, 227-237.	0.7	38
99	Gamma, neutron, and heavy charged ion shielding properties of Er ³⁺ -doped and Sm ³⁺ -doped zinc borate glasses. Open Chemistry, 2022, 20, 130-145.	1.9	38
100	Lithium-fluoro borotellurite glasses: Nonlinear optical, mechanical characteristics and gamma radiation protection characteristics. Radiation Physics and Chemistry, 2022, 190, 109819.	2.8	37
101	Measurement of mass attenuation coefficients, effective atomic numbers, and electron densities for different parts of medicinal aromatic plants in low-energy region. Nuclear Science and Techniques/Hewuli, 2018, 29, 1.	3.4	36
102	Studies on the structural, optical and radiation shielding properties of (50 – x) PbO – 10 WO3–10 Na2O – 10 MgO – (20 + x) B2O3 glasses. Journal of Non-Crystalline Solids, 2019, 513, 159-166.	3.1	36
103	Glass fabrication using ceramic and porcelain recycled waste and lithium niobate: physical, structural, optical and nuclear radiation attenuation properties. Journal of Materials Research and Technology, 2021, 15, 4074-4085.	5.8	36
104	Physical, thermal, optical, structural and nuclear radiation shielding properties of Sm2O3 reinforced borotellurite glasses. Ceramics International, 2021, 47, 6154-6168.	4.8	35
105	An extended assessment of natural radioactivity in the sediments of the mid-region of the Egyptian Red Sea coast. Marine Pollution Bulletin, 2021, 171, 112658.	5.0	35
106	The effective role of La2O3 contribution on zinc borate glasses: radiation shielding and mechanical properties. Applied Physics A: Materials Science and Processing, 2019, 125, 1.	2.3	34
107	Fabrication, physical characteristic, and gamma-photon attenuation parameters of newly developed molybdenum reinforced bismuth borate glasses. Physica Scripta, 2020, 95, 115703.	2.5	34
108	Stuctural, optical and radiation shielding properties of zinc boro-tellurite alumina glasses. Applied Physics A: Materials Science and Processing, 2019, 125, 1.	2.3	33

#	Article	IF	CITATIONS
109	Optical, structural and gamma ray shielding properties of dolomite doped lithium borate glasses for radiation shielding applications. Journal of Non-Crystalline Solids, 2020, 539, 120049.	3.1	33
110	Detailed Inspection of Î ³ -ray, Fast and Thermal Neutrons Shielding Competence of Calcium Oxide or Strontium Oxide Comprising Bismuth Borate Glasses. Materials, 2021, 14, 2265.	2.9	33
111	An experimental evaluation of CdO/PbO-B2O3 glasses containing neodymium oxide: Structure, electrical conductivity, and gamma-ray resistance. Materials Research Bulletin, 2022, 151, 111828.	5.2	33
112	Enhancement of Gamma-ray Shielding Properties in Cobalt-Doped Heavy Metal Borate Glasses: The Role of Lanthanum Oxide Reinforcement. Materials, 2021, 14, 7703.	2.9	33
113	A Systematical Characterization of TeO2–V2O5 Glass System Using Boron (III) Oxide and Neodymium (III) Oxide Substitution: Resistance Behaviors against Ionizing Radiation. Applied Sciences (Switzerland), 2021, 11, 3035.	2.5	32
114	Fabrication, structural, optical, physical and radiation shielding characterization of indium (III) oxide reinforced 85TeO2-(15–x)ZnO-xIn2O3 glass system. Ceramics International, 2021, 47, 27305-27315.	4.8	32
115	Synthesis and structural, optical, physical properties of Gadolinium (III) oxide reinforced TeO2–B2O3–(20-x)Li2O-xGd2O3 glass system. Journal of Alloys and Compounds, 2021, 877, 160302.	5.5	32
116	A closer-look on Copper(II) oxide reinforced Calcium-Borate glasses: Fabrication and multiple experimental assessment on optical, structural, physical, and experimental neutron/gamma shielding properties. Ceramics International, 2022, 48, 6780-6791.	4.8	32
117	Bioactive glasses with TiO2 additive: Behavior characterization against nuclear radiation and determination of buildup factors. Ceramics International, 2020, 46, 10779-10787.	4.8	31
118	Nb2O5-Li2O-Bi2O3-B2O3 novel glassy system: evaluation of optical, mechanical, and gamma shielding parameters. Journal of Materials Science: Materials in Electronics, 2020, 31, 22039-22056.	2.2	31
119	Prediction of mechanical and radiation parameters of glasses with high Bi2O3 concentration. Results in Physics, 2021, 21, 103839.	4.1	31
120	Material characterization of WO3/Bi2O3 substituted calcium-borosilicate glasses: Structural, physical, mechanical properties and gamma-ray resistance competencies. Journal of Alloys and Compounds, 2021, 888, 161419.	5.5	31
121	Experimental and FLUKA evaluation on structure and optical properties and Î ³ -radiation shielding capacity of bismuth borophosphate glasses. Progress in Nuclear Energy, 2022, 148, 104219.	2.9	31
122	Mechanical and nuclear shielding properties of sodium cadmium borate glasses: Impact of cadmium oxide additive. Ceramics International, 2020, 46, 2661-2669.	4.8	30
123	Probing of nuclear radiation attenuation and mechanical features for lithium bismuth borate glasses with improving Bi2O3 content for B2O3Â+ÂLi2O amounts. Results in Physics, 2021, 25, 104246.	4.1	30
124	Mechanical, physical and gamma ray shielding properties of xPbO-(50-x) MoO3–50V2O5 (25 ≤ ≤45Âmo	ol) Tj ETQq 4 :8	0 0 0 rgBT /0
125	Characterization of Ultramafic–Alkaline–Carbonatite complex for radiation shielding competencies: An experimental and Monte Carlo study with lithological mapping. Ore Geology Reviews, 2022, 142, 104735.	2.7	29
	Synthesis and experimental characterization on fast neutron and gamma-ray attenuation properties of		

Synthesis and experimental characterization on fast neutron and gamma-ray attenuation properties of high-dense and transparent Cadmium oxide (CdO) glasses for shielding purposes. Ceramics 4.8 29 International, 2022, 48, 23444-23451.

#	Article	IF	CITATIONS
127	Bi2O3-B2O3-ZnO-BaO-Li2O glass system for gamma ray shielding applications. Optik, 2020, 201, 163525.	2.9	28
128	Newly developed BGO glasses: Synthesis, optical and nuclear radiation shielding properties. Ceramics International, 2020, 46, 11861-11873.	4.8	28
129	Neutron-shielding behaviour investigations of some clay-materials. Nuclear Engineering and Technology, 2019, 51, 1444-1450.	2.3	27
130	Two-step investigation on fabrication and characterization of iron-reinforced novel composite materials for nuclear-radiation shielding applications. Journal of Physics and Chemistry of Solids, 2020, 146, 109604.	4.0	27
131	In-depth survey of nuclear radiation attenuation efficacies for high density bismuth lead borate glass system. Results in Physics, 2021, 23, 104030.	4.1	27
132	Cerium (IV) oxide reinforced Lithium-Borotellurite glasses: A characterization study through physical, optical, structural and radiation shielding properties. Ceramics International, 2022, 48, 1152-1165.	4.8	27
133	Sodium dodecatungstophosphate hydrate-filled polymer composites for nuclear radiation shielding. Materials Chemistry and Physics, 2020, 256, 123667.	4.0	26
134	Comparative evaluation of nuclear radiation shielding properties of xTeO2 + (100–x)Li2O glass system Applied Physics A: Materials Science and Processing, 2020, 126, 1.	^{1.} 2.3	26
135	Shielding features, to non-ionizing and ionizing photons, of FeCr-based composites. Applied Radiation and Isotopes, 2021, 167, 109470.	1.5	26
136	Effect of Heat Treatment on Radiation Shielding Properties of Concretes. Journal of Radiation Protection and Research, 2018, 43, 20-28.	0.6	26
137	Illustration of distinct nuclear radiation transmission factors combined with physical and elastic characteristics of barium boro-bismuthate glasses. Results in Physics, 2021, 31, 105067.	4.1	26
138	Gamma, Fast Neutron, Proton, and Alpha Shielding Properties of Borate Glasses: A Closer Look on Lead (II) Oxide and Bismuth (III) Oxide Reinforcement. Applied Sciences (Switzerland), 2021, 11, 6837.	2.5	25
139	Gamma ray shielding studies on 26.66 B ₂ O ₃ –16GeO ₂ –4Bi ₂ O ₃ –(53.33–x) PbO–xPbF ₂ glass system using MCNPX, Geant4 and XCOM. Materials Research Express, 2018, 5. 095203.	1.6	24
140	CdO-rich quaternary tellurite glasses for nuclear safety purposes: Synthesis and experimental gamma-ray and neutron radiation assessment of high-density and transparent samples. Optical Materials, 2022, 129, 112512.	3.6	24
141	A rapid and direct method for half value layer calculations for nuclear safety studies using MCNPX Monte Carlo code. Nuclear Engineering and Technology, 2022, 54, 3317-3323.	2.3	23
142	Heavy metal oxide (HMO) glasses as an effective member of glass shield family: A comprehensive characterization on gamma ray shielding properties of various structures. Journal of Materials Research and Technology, 2022, 18, 231-244.	5.8	23
143	Investigation of gamma-ray shielding properties of bismuth borotellurite glasses using MCNPX code and XCOM program. Applied Physics A: Materials Science and Processing, 2019, 125, 1.	2.3	22
144	Gamma-Ray Protection Properties of Bismuth-Silicate Glasses against Some Diagnostic Nuclear Medicine Radioisotopes: A Comprehensive Study. Materials, 2021, 14, 6668.	2.9	22

#	Article	IF	CITATIONS
145	Relationship Between Hallux Valgus and Pes Planus: Real or Fiction?. Journal of Foot and Ankle Surgery, 2020, 59, 513-517.	1.0	21
146	Exploring the FTIR, Optical and Nuclear Radiation Shielding Properties of Samarium-Borate Class: A Characterization through Experimental and Simulation Methods. Nanomaterials, 2021, 11, 1713.	4.1	21
147	Investigation of Nanoparticle Effect on Radiation Shielding Property Using Monte Carlo Method. Celal Bayar Universitesi Fen Bilimleri Dergisi, 2016, 12, .	0.5	21
148	Petrology and geochemistry of multiphase post-granitic dikes: A case study from the Gabal Serbal area, Southwestern Sinai, Egypt. Open Chemistry, 2022, 20, 169-181.	1.9	21
149	Iron (III) oxide doped lithium borate glasses: structural and charged particles/photon shielding properties. Journal of Non-Crystalline Solids, 2020, 546, 120281.	3.1	20
150	Relationship between melting-conditions and gamma shielding performance of fluoro-sulfo-phosphate (FPS) glass systems: A comparative investigation. Ceramics International, 2020, 46, 15255-15269.	4.8	20
151	Alkaline phosphate glasses and synergistic impact of germanium oxide (GeO2) additive: Mechanical and nuclear radiation shielding behaviors. Ceramics International, 2020, 46, 16781-16797.	4.8	20
152	An extensive survey of radiographers from the Middle East and India on artificial intelligence integrationÂin radiology practice. Health and Technology, 2021, 11, 1045-1050.	3.6	20
153	Novel Cu/Zn Reinforced Polymer Composites: Experimental Characterization for Radiation Protection Efficiency (RPE) and Shielding Properties for Alpha, Proton, Neutron, and Gamma Radiations. Polymers, 2021, 13, 3157.	4.5	19
154	Comparative assessment of fast and thermal neutrons and gamma radiation protection qualities combined with mechanical factors of different borate-based glass systems. Results in Physics, 2022, 37, 105527.	4.1	19
155	Borax effect on gamma and neutron shielding features of lithium borate glasses: an experimental and Monte Carlo studies. Materials Research Express, 2019, 6, 115217.	1.6	18
156	Analysis of red mud doped Bi2O3-B2O3-BaO glasses for application as glass solder in radiation shield repair using MCNPX simulation. Ceramics International, 2019, 45, 7619-7626.	4.8	18
157	Promising applicable heterometallic Al2O3/PbO2 nanoparticles in shielding properties. Journal of Materials Research and Technology, 2020, 9, 13956-13962.	5.8	18
158	Characterization of optical and radiation shielding behaviors of ferric oxide reinforced bismuth borate glass. Physica Scripta, 2021, 96, 075801.	2.5	18
159	Erbium (III)- and Terbium (III)-containing silicate-based bioactive glass powders: physical, structural and nuclear radiation shielding characteristics. Applied Physics A: Materials Science and Processing, 2021, 127, 1.	2.3	18
160	Cadmium oxide reinforced 46V2O5–46P2O5–(8â^'x)B2O3–xCdO semiconducting oxide glasses and resistance behaviors against ionizing gamma rays. Journal of Materials Research and Technology, 2021, 13, 2336-2349.	5.8	18
161	Validation of MCNPX with Experimental Results of Mass Attenuation Coefficients for Cement, Gypsum and Mixture. Journal of Radiation Protection and Research, 2017, 42, 154-157.	0.6	18
162	B2O3-Bi2O3-Li2O3-Cr2O3 glasses: fabrication, structure, mechanical, and gamma radiation shielding qualities. Journal of the Australian Ceramic Society, 2021, 57, 1057-1069.	1.9	17

#	Article	IF	CITATIONS
163	Novel HMO-Glasses with Sb2O3 and TeO2 for Nuclear Radiation Shielding Purposes: A Comparative Analysis with Traditional and Novel Shields. Materials, 2021, 14, 4330.	2.9	17
164	Exploration of material characteristics of tantalum borosilicate glasses by experimental, simulation, and theoretical methods. Journal of Physics and Chemistry of Solids, 2021, 159, 110282.	4.0	17
165	Synthesis and characterization of waste CRT glasses through physical, optical and structural properties: A comprehensive study on recycling. Optik, 2021, 248, 168167.	2.9	17
166	Mechanical properties, elastic moduli, transmission factors, and gamma-ray-shielding performances of Bi ₂ O ₃ –P ₂ O ₅ –B ₂ O ₃ –V <sub quaternary glass system. Open Chemistry, 2022, 20, 314-329.</sub 	> <u>1</u> >2(⊃ ¹⁷ sub>5
167	Assessment of MRI technologists in acceptance and willingness to integrate artificial intelligence into practice. Radiography, 2021, 27, S83-S87.	2.1	16
168	WS2/bioactive glass composites: Fabrication, structural, mechanical and radiation attenuation properties. Ceramics International, 2021, 47, 29739-29747.	4.8	16
169	Computed tomography radiation doses for common computed tomography examinations: a nationwide dose survey in United Arab Emirates. Insights Into Imaging, 2020, 11, 88.	3.4	16
170	Newly Developed Vanadium-Based Glasses and Their Potential for Nuclear Radiation Shielding Aims: A Monte Carlo Study on Gamma Ray Attenuation Parameters. Materials, 2021, 14, 3897.	2.9	15
171	Analysis of physical and mechanical traits and nuclear radiation transmission aspects of Gallium(III) trioxide constituting Bi2O3-B2O3 glasses. Results in Physics, 2021, 30, 104899.	4.1	15
172	Transmission Factor (TF) Behavior of Bi2O3–TeO2–Na2O–TiO2–ZnO Glass System: A Monte Carlo Simulation Study. Sustainability, 2022, 14, 2893.	3.2	15
173	Physical, structural, mechanical and radiation shielding features of waste pharmaceutical glasses doped with Bi2O3. Optik, 2022, 261, 169108.	2.9	15
174	Impact of molybdenum on optical, structure properties and gamma radiation shielding parameters of bor-ophosphate glass: Intensive experiment investigations. Radiation Physics and Chemistry, 2022, 198, 110140.	2.8	15
175	Fabrication, physical, structure characteristics, neutron and radiation shielding capacityÂof high-density neodymio-cadmium lead-borate glasses: Nd2O3/CdO/PbO/B2O3/Na2O. Applied Physics A: Materials Science and Processing, 2022, 128, .	2.3	15
176	Synthesis and characterization of vanadium(V) oxide reinforced calcium-borate glasses: Experimental assessments on Al2O3/BaO2/ZnO contributions. Journal of Non-Crystalline Solids, 2022, 580, 121397.	3.1	14
177	Gallium (III) oxide reinforced novel heavy metal oxide (HMO) glasses: A focusing study on synthesis, optical and gamma-ray shielding properties. Ceramics International, 2022, 48, 14261-14272.	4.8	14
178	Calculation of gamma-ray attenuation properties of some antioxidants using Monte Carlo simulation method. Biomedical Physics and Engineering Express, 2018, 4, 057001.	1.2	13
179	Fabrication, optical characteristic, and nuclear radiation shielding properties of newly synthesised PbO–GeO2 glasses. Applied Physics A: Materials Science and Processing, 2020, 126, 1.	2.3	13
180	Structural and nuclear shielding qualities of B2O3–PbO–Li2O glass system with different Ag2O substitution ratios. Radiation Physics and Chemistry, 2021, 179, 109262.	2.8	13

#	Article	IF	CITATIONS
181	Optical and nuclear radiation protection characteristics of lithium bismo-borate glasses: Role of ZrO2 substitution. Radiation Physics and Chemistry, 2021, 183, 109428.	2.8	13
182	Synthesis and dielectric relaxation behavior of 55B2O3–15SiO2– 30Na2O: WO3 glass system. Ceramics International, 2021, 47, 20201-20209.	4.8	13
183	Mechanical Properties, Elastic Moduli, and Gamma Radiation Shielding Properties of Some Zinc Sodium Tetraborate Glasses: A Closer Look at ZnO/CaO Substitution. Journal of Electronic Materials, 2021, 50, 6844-6853.	2.2	13
184	Synthesis and characterization of newly developed phosphate-based glasses through experimental gamma-ray and neutron spectroscopy methods: Transmission and dose rates. Ceramics International, 2022, 48, 13842-13849.	4.8	13
185	The significant role of WO3 on high-dense BaO–P2O3 glasses: transmission factors and a comparative investigation using commercial and other types of shields. Applied Physics A: Materials Science and Processing, 2022, 128, 1.	2.3	13
186	Determining the gamma-ray parameters for BaO–ZnO–B ₂ O ₃ glasses using MCNP5 code: a comparison study. Radiation Effects and Defects in Solids, 2018, 173, 510-525.	1.2	12
187	Synergistic effects of quercetin and selenium on oxidative stress in endometrial adenocarcinoma cells. Bratislava Medical Journal, 2019, 120, 449-455.	0.8	12
188	<p>Effectiveness of Breast and Eye Shielding During Cervical Spine Radiography: An Experimental Study</p> . Risk Management and Healthcare Policy, 2020, Volume 13, 697-704.	2.5	12
189	Linear/nonlinear optical parameters along with photon attenuation effectiveness of Dy3+ ions doped zinc-aluminoborosilicate glasses. Physica Scripta, 0, , .	2.5	12
190	A Closer Look on Nuclear Radiation Shielding Properties of Eu3+ Doped Heavy Metal Oxide Glasses: Impact of Al2O3/PbO Substitution. Materials, 2021, 14, 5334.	2.9	12
191	Statistical analysis on the radiological assessment and geochemical studies of granite rocks in the north of Um Taghir area, Eastern Desert, Egypt. Open Chemistry, 2022, 20, 254-266.	1.9	12
192	Synthesis and structural, electrical, optical, and gamma-ray attenuation properties of ZnO-multi-walled carbon nanotubes (MWCNT) composite separately incorporated with CdO, TiO2, and Fe2O3. Ceramics International, 2022, 48, 16251-16262.	4.8	12
193	Nuclear shielding performances of borate/sodium/potassium glasses doped with Sm3+ ions. Journal of Materials Research and Technology, 2022, 18, 1424-1435.	5.8	12
194	Structural and photon attenuation properties of different types of fiber post materials for dental radiology applications. Results in Physics, 2019, 13, 102354.	4.1	11
195	Improvement of radiation shielding properties of some tellurovanadate based glasses. Physica Scripta, 2020, 95, 035402.	2.5	11
196	TOWARD NATIONAL CT DIAGNOSTIC REFERENCE LEVELS IN THE UNITED ARAB EMIRATES: A MULTICENTER REVIEW OF CT DOSE INDEX AND DOSE LENGTH PRODUCT. Radiation Protection Dosimetry, 2020, 190, 243-249.	0.8	11
197	Scanning electron microscopy (SEM), energy-dispersive X-ray (EDX) spectroscopy and nuclear radiation shielding properties of [α-Fe3+O(OH)]-doped lithium borate glasses. Applied Physics A: Materials Science and Processing, 2020, 126, 1.	2.3	11
198	Mechanical and nuclear radiation shielding properties of different boro-tellurite glasses: a comprehensive investigation on large Bi ₂ O ₃ concentration. Physica Scripta, 2020, 95, 085701.	2.5	11

#	Article	IF	CITATIONS
199	Optical, structural and nuclear radiation shielding properties of Li2B4O7 glasses: effect of boron mineral additive. Applied Physics A: Materials Science and Processing, 2020, 126, 1.	2.3	11
200	Effect of Ag2O substituted in bioactive glasses: a synergistic relationship between antibacterial zone and radiation attenuation properties. Journal of Materials Research and Technology, 2021, 13, 2194-2201.	5.8	11
201	The significant role of CeO ₂ content on the radiation shielding performance of Fe ₂ O ₃ -P ₂ O ₅ glass-ceramics: Geant4 simulations study. Physica Scripta, 2021, 96, 115305.	2.5	11
202	Optical and physical behaviours of newly developed germanium-tellurium (GeTe) glasses: a comprehensive experimental and in-silico study with commercial glasses and ordinary shields. Journal of Materials Science: Materials in Electronics, 2021, 32, 22953-22973.	2.2	11
203	Fabrication, physical, structural, and optical investigation of cadmium lead-borate glasses doped with Nd3+ ions: AnAexperimental study. Journal of Materials Science: Materials in Electronics, 2022, 33, 1877-1887.	2.2	11
204	A thorough examination of gadolinium (III)-containing silicate bioactive glasses: synthesis, physical, mechanical, elastic and radiation attenuation properties. Applied Physics A: Materials Science and Processing, 2022, 128, 1.	2.3	11
205	Transmission factors, mechanical, and gamma ray attenuation properties of barium-phosphate-tungsten glasses: Incorporation impact of WO3. Optik, 2022, 267, 169643.	2.9	11
206	Spectroscopic and thermal analysis of lead-free multipurpose radiation shielding glasses. Ceramics International, 2019, 45, 5332-5338.	4.8	10
207	Comparison of gamma and neutron shielding competences of Fe–Cu- and brass-added Portland cement pastes: an experimental and Monte Carlo study. Applied Physics A: Materials Science and Processing, 2020, 126, 1.	2.3	10
208	Synergistic effect of serpentine mineral on Li2B4O7 glasses: optical, structural and nuclear radiation shielding properties. Applied Physics A: Materials Science and Processing, 2020, 126, 1.	2.3	10
209	An experimental investigation on structural, mechanical and physical properties of Strontium–Silicon Borate glass system through Bismuth-Aluminum substitution. Optical Materials, 2021, 117, 111124.	3.6	10
210	The Impact of PbF2-Based Glasses on Radiation Shielding and Mechanical Concepts: An Extensive Theoretical and Monte Carlo Simulation Study. Journal of Inorganic and Organometallic Polymers and Materials, 2021, 31, 3934-3942.	3.7	10
211	An in-depth investigation from mechanical durability to structural and nuclear radiation attenuation properties: B ₂ O ₃ –Na ₂ O–Bi ₂ O ₃ –Nb ₂ Og–Bi ₂ O ₃ –Nb ₂ O	< sub >5 </td <td>10 suD≻</td>	10 suD≻
212	Optimizing the shielding properties of strength-enhanced concrete containing marble. Papers in Physics, 0, 12, 120005.	0.2	10
213	Newly synthesized NiCoFeCrW High-Entropy Alloys (HEAs): Multiple impacts of B4C additive on structural, mechanical, and nuclear shielding properties. Intermetallics, 2022, 146, 107593.	3.9	10
214	13-93B3 Bioactive glasses containing Ce3+, Ga3+ and V5+: dose rate and gamma radiation characteristic for medical purposes. Applied Physics A: Materials Science and Processing, 2021, 127, 1.	2.3	9
215	Mechanical, structural and nuclear radiation shielding competencies of some tellurite glasses reinforced with molybdenum trioxide. Physica Scripta, 2021, 96, 045702.	2.5	9
216	Multiple characterization of some glassy-alloys as photon and neutron shields: In-silico Monte Carlo investigation. Materials Research Express, 2021, 8, 035202.	1.6	9

#	Article	IF	CITATIONS
217	In-Silico Monte Carlo Simulation Trials for Investigation of V2O5 Reinforcement Effect on Ternary Zinc Borate Glasses: Nuclear Radiation Shielding Dynamics. Materials, 2021, 14, 1158.	2.9	9
218	Developed selenium dioxide-based ceramics for advanced shielding applications: Au2O3 impact on nuclear radiation attenuation. Results in Physics, 2021, 24, 104099.	4.1	9
219	Specific Absorption Rate Dependency on the Co2+ Distribution and Magnetic Properties in CoxMn1-xFe2O4 Nanoparticles. Nanomaterials, 2021, 11, 1231.	4.1	9
220	Mechanical properties and elastic moduli, as well as gamma-ray attenuation abilities: A wide-ranging investigation into calcium/sodium/phosphate glasses. Journal of the Australian Ceramic Society, 2021, 57, 1309-1319.	1.9	9
221	Fast Neutron and Gamma-Ray Attenuation Properties of Some HMO Tellurite-Tungstate-Antimonate Glasses: Impact of Sm3+ Ions. Applied Sciences (Switzerland), 2021, 11, 10168.	2.5	9
222	Fabrication of newly developed tungsten III-oxide glass family: Physical, structural, mechanical, radiation shielding effectiveness. Optik, 2022, 259, 169025.	2.9	9
223	Occupational radiation dose assessment for nuclear medicine workers in Turkey: A comprehensive investigation. Journal of King Saud University - Science, 2022, 34, 102005.	3.5	9
224	Synergistic effect of boron nitride and graphene nanosheets on behavioural attitudes of polyester matrix: Synthesis, experimental and Monte Carlo simulation studies. Diamond and Related Materials, 2022, 126, 109095.	3.9	9
225	Diagnostic and therapeutic radioisotopes in nuclear medicine: Determination of gamma-ray transmission factors and safety competencies of high-dense and transparent glassy shields. Open Chemistry, 2022, 20, 517-524.	1.9	9
226	Radiation shielding parameters of some antioxidants using Monte Carlo method. Journal of Biological Physics, 2018, 44, 579-590.	1.5	8
227	New shielding ZnO-PbO-TeO2 glasses. Optik, 2021, 243, 167483.	2.9	8
228	Structural characterization and gamma-ray attenuation properties of rice-like α-TeO2 crystalline microstructures (CMS) grown rapidly on free surface of tellurite-based glasses. Journal of Materials Research and Technology, 2022, 16, 1179-1189.	5.8	8
229	Evaluating the optical and gamma-ray protection properties of bismo-tellurite sodium titanium zinc glasses. Journal of the Australian Ceramic Society, 2022, 58, 851-866.	1.9	8
230	Structural, optical, mechanical and simulating the gamma-ray shielding competencies of novel cadmium bismo-borate glasses: The impact of bismuth oxide. Journal of Materials Science: Materials in Electronics, 2021, 32, 24381-24393.	2.2	7
231	Adult Patient Radiation Doses with Multislice Computed Tomography Exam: MSCT Standard Protocols. Acta Physica Polonica A, 2017, 132, 1126-1127.	0.5	7
232	Monte Carlo Simulation for Distance and Absorbed Dose Calculations in a PET-CT Facility by Using MCNP-X. Journal of Communication and Computer, 2016, 13, .	0.1	7
233	Impact of Eye and Breast Shielding on Organ Doses During Cervical Spine Radiography: Design and Validation of MIRD Computational Phantom. Frontiers in Public Health, 2021, 9, 751577.	2.7	7
234	Refinement of optical/structural features and neutron/gamma-ray protecting capability of P2O5–Li2O–BaO phosphate glass system by adding Bi2O3. Progress in Nuclear Energy, 2022, 145, 104114.	2.9	7

#	Article	IF	CITATIONS
235	Dielectric, structural, optical and radiation shielding properties of newly synthesized CaO–SiO2–Na2O–Al2O3 glasses: experimental and theoretical investigations on impact of Tungsten(III) oxide. Applied Physics A: Materials Science and Processing, 2022, 128, 1.	2.3	7
236	Multiple Assessments on the Gamma-Ray Protection Properties of Niobium-Doped Borotellurite Glasses: A Wide Range Investigation Using Monte Carlo Simulations. Science and Technology of Nuclear Installations, 2022, 2022, 1-17.	0.8	7
237	<p>Radiography Advanced Practice in the United Arab Emirates: The Perceptions and Readiness of Mammographers</p> . Journal of Multidisciplinary Healthcare, 2020, Volume 13, 753-758.	2.7	6
238	(59.5–x) P2O5–30Na2O–10Al2O3–0.5CoO–xNd2O3 glassy system: an experimental investigation on structural and gamma-ray shielding properties. Applied Physics A: Materials Science and Processing, 2020, 126, 1.	2.3	6
239	FTIR, structural and radiation attenuation properties of amalgam dental composites for medical applications. Materials Chemistry and Physics, 2020, 253, 123261.	4.0	6
240	Characterization of synthesized xBaO-(40-x)Li2O-60B2O3 glass system: a multi-dimensional research on optical and physical properties. Journal of Materials Science: Materials in Electronics, 2021, 32, 16990-17008.	2.2	6
241	Performance of Boron-Carbide as Radiation Shielding. Acta Physica Polonica A, 2015, 128, B-335-B-337.	0.5	6
242	Thermal and Optical Characteristics of Synthesized Sand/CeO2 Glasses: Experimental Approach. Journal of Electronic Materials, 2022, 51, 2070-2076.	2.2	6
243	Molecular Polar Surface Area, Total Solvent Accessible Surface Area (SASA), Heat of Formation, and Gamma-Ray Attenuation Properties of Some Flavonoids. Frontiers in Physics, 2022, 10, .	2.1	6
244	Boron nitride nanosheet-reinforced WNiCoFeCr high-entropy alloys: the role of B4C on the structural, physical, mechanical, and radiological shielding properties. Applied Physics A: Materials Science and Processing, 2022, 128, .	2.3	6
245	An extensive study on nuclear shielding performance and mass stopping powerÂ(MSP)/projected rangesÂ(PR) of some selected granite samples. Radiation Effects and Defects in Solids, 2021, 176, 320-340.	1.2	5
246	Nitrogen Source, an Important Determinant of Fatty Acid Accumulation and Profile in Scenedesmus obliquus. Acta Physica Polonica A, 2016, 130, 428-433.	0.5	5
247	Farklı Türdeki Betonların Kütle Zayıflatma Katsayılarının Monte Carlo Metodu ile Belirlenmesi. European Journal of Science and Technology, 0, , 591-598.	0.5	5
248	Investigation of the elastic moduli, optical characteristics, and ionizing radiation attenuation capacity of specific strontium borosilicateÂglasses. Journal of the Australian Ceramic Society, 2022, 58, 495-510.	1.9	5
249	Radiation shielding properties for titanium dioxide added composites. Emerging Materials Research, 2022, 11, 1-7.	0.7	5
250	Calculation of NaI(Tl) detector efficiency using ²²⁶ Ra, ²³² Th, and ⁴⁰ K radioisotopes: Three-phase Monte Carlo simulation study. Open Chemistry, 2022, 20, 541-549.	1.9	5
251	Radiation protection characteristics of nano-concretes against photon and neutron beams. , 2020, , 447-460.		4
252	Structural, surface morphology and radiation shielding properties of barium ferrite powder. Physica Scripta, 2021, 96, 095805.	2.5	4

#	Article	IF	CITATIONS
253	Municipal waste slag for dyes photocatalytic and metal recovery applications through structural analysis and experimental characterization. International Journal of Energy Research, 2021, 45, 17691-17708.	4.5	4
254	Synthesis, physical, linear optical and nuclear radiation shielding characteristics of B2O3–BaO–PbO–SrO2 glasses. Journal of Materials Science: Materials in Electronics, 2021, 32, 18163-18177.	2.2	4
255	Tailoring the structuralism in xBaO·(30–x)Li ₂ O·70B ₂ O ₃ glasses for highly efficient shields of Gamma radiation and neutrons attenuators. Physica Scripta, 2021, 96, 125308.	2.5	4
256	Assessment of absorbed dose for Zr-89, Sm-153 and Lu-177 medical radioisotopes: IDAC-Dose2.1 and OLINDA experience. Applied Radiation and Isotopes, 2021, 176, 109841.	1.5	4
257	An Artificial Neural Network-Based Estimation of Bremsstarahlung Photon Flux Calculated by MCNPX. Acta Physica Polonica A, 2017, 132, 967-969.	0.5	4
258	Gamma Shielding Properties of Erbium Zinc Tellurite Glass System Using Monte Carlo Method. Journal of Testing and Evaluation, 2020, 48, 20180123.	0.7	4
259	Trivalent Ions and Their Impacts on Effective Conductivity at 300 K and Radio-Protective Behaviors of Bismo-Borate Glasses: A Comparative Investigation for Al, Y, Nd, Sm, Eu. Materials, 2021, 14, 5894.	2.9	4
260	Coronavirus Disease 2019 Strategies, Examination Details, and Safety Procedures for Diagnostic Radiology Facilities: An Extensive Multicenter Experience in Istanbul, Turkey. Journal of Radiology Nursing, 2021, 40, 172-178.	0.4	4
261	Analysis of the Radiological, Mineralogical and Long-Term Sustainability of Several Commercial Aswan Granites Used as Building Materials. Sustainability, 2022, 14, 3553.	3.2	4
262	Mechanical properties as well as gamma-ray attenuation competence: a wide-ranging examination into Tb3+ doped boro-germanate-aluminiophosphate (BGAP) glasses. Journal of Materials Research and Technology, 2022, 18, 5062-5074.	5.8	4
263	Gamma ray shielding properties of CeO2-added hydroxyapatite composite. Journal of the Australian Ceramic Society, 2022, 58, 1209-1217.	1.9	4
264	Diagnostic Performance of Machine Learning Models Based on ¹⁸ F-FDG PET/CT Radiomic Features in the Classification of Solitary Pulmonary Nodules. Molecular Imaging and Radionuclide Therapy, 2022, 31, 82-88.	0.7	4
265	Lead exposure in clinical imaging – The elephant in the room. European Journal of Radiology, 2020, 131, 109210.	2.6	3
266	The impact of Nd3+ ions on linear/nonlinear and the ionizing radiation attenuation parameters of TeO2-PbO-Y2O3 glasses. Journal of Materials Science: Materials in Electronics, 2021, 32, 17200-17219.	2.2	3
267	On B2O3/Bi2O3/Na2O/Gd2O3 glasses: synthesis, structure, physical characteristics, and gamma-ray attenuation competence. Applied Physics A: Materials Science and Processing, 2021, 127, 1.	2.3	3
268	Binary contributions of Dy3+ ions on the mechanical and radiation resistance properties of oxyfluoroborotellurite Dyx-glasses. Journal of Materials Research and Technology, 2022, 18, 820-829.	5.8	3
269	Gamma-ray attenuation properties of boron carbide in radiological energy range using MCNPX code. AIP Conference Proceedings, 2018, , .	0.4	2
270	Comparison of Radiation dose and Image Quality in Head CT Scans Among Multidetector CT Scanners. Radiation Protection Dosimetry, 2021, 196, 10-16.	0.8	2

#	Article	IF	CITATIONS
271	IMPACT OF RADIATION FIELD SIZE ON ABSORBED ORGAN DOSES IN NEONATES UNDERGOING CHEST RADIOGRAPHY IN AN ANTERIOR–POSTERIOR PROJECTION: A MONTE CARLO SIMULATION STUDY. Radiation Protection Dosimetry, 2022, 198, 44-52.	0.8	2
272	Response to letter to Editor: Medical Image Analyst: A Radiology Career Focused on Comprehensive Quantitative Imaging Analytics to Improve Healthcare. Academic Radiology, 2022, 29, 171.	2.5	1
273	Computed Tomography Routine Examinations and the Related Risk of Cancer. Acta Physica Polonica A, 2016, 130, 409-411.	0.5	1
274	Quantitative Characteristic X-Ray Analysis for Different Compound Samples by Using Monte Carlo Method. Acta Physica Polonica A, 2017, 132, 439-441.	0.5	1
275	Assessment of MCNPX Monte Carlo Code for Absorbed Dose Calculations in Mammogarphy Examination. Afyon Kocatepe University Journal of Sciences and Engineering, 2017, 17, 48-55.	0.2	1
276	Radiation Protection in PET Room. Acta Physica Polonica A, 2015, 128, B-375-B-378.	0.5	1
277	ESTIMATED RADIATION RISKS, CLINICAL FACTORS AND PATIENT DOSE IN MAMMOGRAPHY. , 0, , .		1
278	ANALYSIS OF FILTERING MATERIAL AND ITS EFFECT ON X-RAY FEATURES BY USING MONTE CARLO METHOD FOR MEDICAL IMAGING APPLICATIONS. , 0, , .		1
279	Comparative study on application of 177Lu-labeled rituximab, tetulomab, cetuximab and huA33 monoclonal antibodies to targeted radionuclide therapy. Biomedical Physics and Engineering Express, 2021, 7, 015015.	1.2	1
280	A Comprehensive Evaluation of the Attenuation Characteristics of Some Sliding Bearing Alloys under 0.015–15 MeV Gamma-Ray Exposure. Materials, 2022, 15, 2464.	2.9	1
281	Corrigendum to "Statistical analysis on the radiological assessment and geochemical studies of granite rocks in the north of Um Taghir area, Eastern Desert, Egypt― Open Chemistry, 2022, 20, 330-330.	1.9	1
282	Four-phases characterization of synthesised CeO2 thin films: Effect of molarity on structural, optical, physical properties and gamma-ray attenuation parameters. Ceramics International, 2022, 48, 25041-25048.	4.8	1
283	Radiation interaction parameters of dosimetric importance for some commonly used compensators in IMRT using Monte Carlo simulation code. Journal of Radiological Protection, 2018, 38, 1321-1343.	1.1	0
284	COMPARISON STUDY OF CLINICAL MEASUREMENTS AND MONTE CARLO METHOD ON RADIATION DOSE RATE CHANGES BY DISTANCE IN COMPUTERIZED TOMOGRAPHY (CT) FACILITY. , 0, , .		0
285	A Prediction Study on Bremsstrahlung Photon Flux of Tungsten as a Radiological Anode Material by using MCNPX and ANN Modeling. Acta Physica Polonica A, 2017, 132, 433-435.	0.5	0
286	Effect of Humeral Locking Plate System on Absorbed Energy in Breast Tissue with Different Radiological Energies Using MCNPX Code. Journal of Testing and Evaluation, 2021, 49, 329-337.	0.7	0
287	Determination of Gamma-Ray Shielding Parameters for Concretes and Dosimeters Using MCNPX. Journal of Nuclear Physics Material Sciences Radiation and Applications, 2020, 8, 73-79.	0.2	0
288	Corrigendum to "Petrology and geochemistry of multiphase post-granitic dikes: A case study from the Gabal Serbal area, Southwestern Sinai, Egypt― Open Chemistry, 2022, 20, 297-298.	1.9	0

#	Article	IF	CITATIONS
289	Calculation of gamma-ray buildup factors for some medical materials. Emerging Materials Research, 2022, 11, 1-9.	0.7	0